Manufacturing Rev. **10**, 3 (2023)

https://doi.org/10.1051/mfreview/2023001

Manufacturing Review
Available online at:
https://mfr.edp-open.org

RESEARCH ARTICLE
OPEN ACCESS

Microstructure, physical, tensile and wear behaviour of B_4C particles reinforced Al7010 alloy composites

Kotresha Mydur[1,*], Mahendra Kumar S.[1], Madeva Nagaral[2], Virupaxi Auradi[3], Bharath V.[4] and Sudarshan T.A.[5]

[1] Department of Mechanical Engineering, RV College of Engineering, Visvesvaraya Technological University, Bangalore 560074, Karnataka, India
[2] Aircraft Research and Design Centre, Hindustan Aeronautics Limited, Bangalore 560037, Karnataka, India
[3] Department of Mechanical Engineering, Siddaganaga Institute of Technology, Visvesvaraya Technological University, Tumakuru 572103, Karnataka, India
[4] Department of Mechanical Engineering, RNS Institute of Technology, Visvesvaraya Technological University, Bangalore 560098, Karnataka, India
[5] Department of Mechanical Engineering, New Horizon College of Engineering, Bangalore 560103, Karnataka, India

Received: 20 October 2022 / Accepted: 29 December 2022

Abstract. In the present study looked into how incorporating B_4C particles with a size range of 20–25 microns would affect the mechanical, wear and physical properties of composites made from Al7010 alloy. The stir cast method accounted for of the total production of B_4C composites. Different mechanical properties, such as hardness, tensile behaviour, wear and density, were measured and analysed for these synthetic composites. Microstructure was characterised by scanning electron microscopy and X-ray diffraction analysis to determine the distribution and phases of particles smaller than a micron. Wear tests were conducted on all the samples at varying loads and speeds. Hardness and tensile strength of Al7010 alloy were improved by adding B_4C particles sized 20–25 microns, with only a minor decrease in elongation. Further, as B_4C particles accumulated, the density of the Al7010 alloy decreased. SEM examination revealed a wide range of fracture behaviours upon tensile stress. Load and sliding speeds affected the wear behaviour of Al7010 alloy and its composites.

Keywords: Al7010 alloy / B_4C / microstructure / hardness / tensile behaviour / fractography / wear

1 Introduction

With their exceptional quality and wear and fatigue resistance compared to traditional unreinforced materials, metal composites based on aluminium alloys have the potential to revolutionise aviation and defence applications [1]. Due to the movement of the load amongst the lattice and earthworks, Al-based MMCs require an enriched interfacial bond among Al grid and fortifications, which dictates the mechanical properties of the composites [2,3].

Support material inserted into the metal increases the specific strength, stiffness, creep, and fatigue compared to standard engineering materials. Particle MMCs (fortified), short fibre supported (fortified), and continuous fibre strengthened and layered MMCs (fortified) can all be classified according to the support materials they are made from [4]. Preliminary studies have shown that the use of consistent fiber-enhanced MMC has been stymied by the high assembling costs of the fortification strands and the arduous assembly processes. As a result, their use has been restricted to the military and other extremely specialised fields. There has been a delay in the commercialization of fiber-strengthened MMCs despite the fact that these fortified MMCs have been shown to have superior thermal stability compared to particulate fortified materials [5,6]. Because of their easy formability and low cost, particulate MMCs have recently been used in a variety of construction applications. Indeed, PAMCs have proven to be an excellent choice for a wide range of automotive and aerospace applications. These include braking mechanisms for trains as well as automobiles; gas turbine motors; helicopter engines; military aircraft and so on [7].

Wear resistance, stiffness, and indicated strength are all achieved by combining various types of particulate fortifications such as Al_2O_3, B_4C, Fly ash, ZrO_2, and so on with aluminium [8,9]. With high modulus and resistance to thermal stress, these ceramic particles are widely used as a

* e-mail: kotresha_mydur@rediffmail.com

support in a variety of development materials. Improved rigidity of the composites was achieved by increasing the amount of aluminium amalgam particles in the mixture. B_4C improves the hardness and wear resistance of aluminum-boron carbide metal grid composites by acting as a lubricating film on the contact surface and with low warm extension. B_4C improves the mechanical, wear resistance, and hardness of the material at high temperatures. Aluminum metal composites are primarily used in aircraft and vehicles because of their high explicit quality and strength as well as their excellent resistance to wear and tear.

This is because the mechanical requirements and desired properties of aluminium composites are closely tied to the preparation technique, and thus, the choice of creation process is critical [10,11]. Delivery of aluminium composites is hindered by higher support material costs, non-homogeneous fortification dispersion in the framework, and sometimes higher venture costs. Composites' expanding range of uses depends on a well-thought-out assembly technique [12]. Stir casting, compo casting, infiltration, and powder metallurgy are the primary manufacturing techniques for mass metal composites [13].

A two-stage reinforcement addition method was used to make Al7010 composites by adding 4 and 8 wt.% of 20–25 micron sized B_4C particles. A further study was done on the mechanical and wear properties of B_4C composites made of Al7010 alloy.

2 Experimental details

Stir casting was used to create metal composites containing 4 and 8 wt.% of B_4C particulates with a diameter of 20–25 microns. Al7010 was used as the main material, while B_4C particles with a diameter of 20–25 microns were taken as reinforcements, as shown in Figure 1. Table 1 lists the alloy's chemical composition for the current investigation.

Al7010 alloy with 20–25 micron-sized reinforced B_4C composites is produced using the liquid technique on stir casting method. Al7010 alloy metal blocks of a specified mass are loaded into the electric furnace and heated to the molten state. Al7010 alloy has a melting point of 660 °C, but is superheated to 750 °C in this process. The melting and superheated temperatures are recorded after being measured using thermocouples with the appropriate temperature range. About three minutes of degassing with solid hexachloroethane (C_2Cl_6) is required to remove the gas from the crucible's superheated molten metal. The molten metal is stirred using a bladed fan type steel rotor coated with zirconia ceramic material. About 65% of the crucible is filled with molten metal, and the stirrer is submerged in the molten metal and rotated at approximately 300 rpm to create vortices in the metal. The preheated B_4C particles added into the Al molten material. Stirring continues until the Al7010 alloy matrix and B_4C reinforce particulates are completely wettable, at which point the interfacial shear strength is established as a result. To make the Al7010 alloy with a 4% composite content, the molten metal of Al7010 matrix and B_4C is poured into cast iron moulds with dimensions of 120 mm in length and with a diameter of 15 mm. When producing composites with B_4C particulates, the same method is used, regardless of the percentage of composites. Figure 2 shows the composites of Al7010 alloy and B_4C that were prepared. Figure 3 is showing the flow chart of the work.

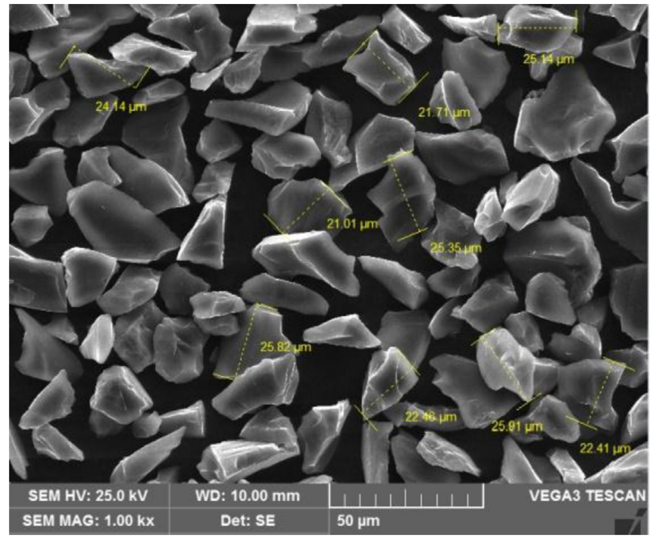

Fig. 1. SEM micrograph of 20–25 micron sized B_4C particles.

Table 1. Chemistry of Al7010 alloy by wt.%.

Zn	Mg	Si	Fe	Cu	Ni	Mn	Cr	Al
6.70	2.60	0.12	0.15	2.0	0.05	0.10	0.05	Balance

Fig. 2. Prepared Al7010 alloy B_4C composite.

Scanning electronic microscopes are used to inspect the microstructure of the Al7010 alloy, determining the even distribution of reinforcement particles. Al7010 and Al7010 alloy with varying wt.% of B_4C reinforced composites microstructure images are taken. Microstructure specimens have a 15 mm diameter and a 5 mm height.

The densities of the Al7010 alloy with B_4C composites were analysed. According to the rule of mixture, the theoretic values were calculated, and the experimental densities used the standard weight method.

The hardness test sample is machined as per ASTM standard E10 [14]. A Brinell hardness tester machine is used to measure the hardness. There is no roughness to the specimen's surface. The specimen has been subjected to a 250 kg load and a 5 mm ball indentation has been taken. The average of five indentation marks is taken into consideration.

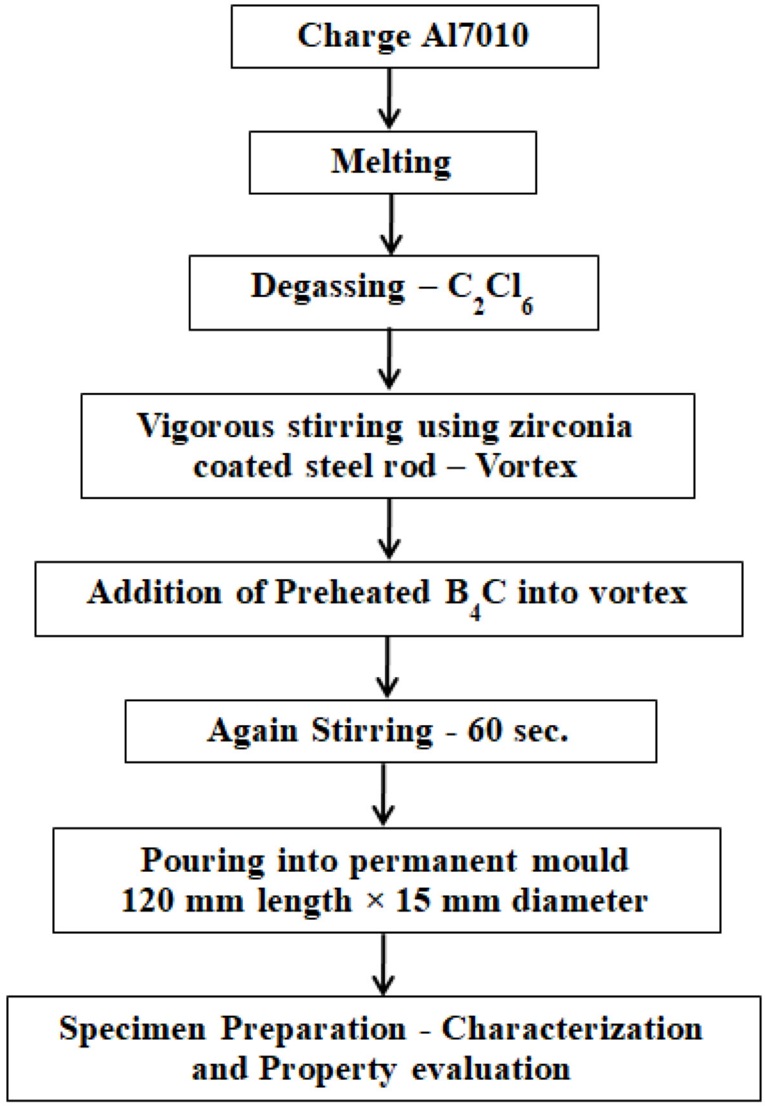

Fig. 3. Process flow chart of the research work.

Machined as per ASTM E8 standard [15] for tensile features of as-cast Al7010 with varying wt.% B_4C particulate reinforced composites. It is used to measure the tensile strength of Al7010 and B_4C composites under unidirectional tension, as well as to examine the effect of even dissemination on its behaviour. The specimen has an overall length of 104 mm, a gauge length of 45 mm, and a gauge diameter of 9 mm. The ultimate, yield, and elongation of a material can be determined by conducting this tensile test.

To investigate wear behaviour, pin-on-disc wear tests were conducted (DUCOM, TR-20LE). Wear tests of 30 mm height and diameter of 8 mm were performed on both base and composites in accordance with ASTM G99 standards [16]. The counter disc in the wear machine was made from EN32 steel. Before testing can begin, the disc and test pin surface are cleaned with acetone liquid. Experimentations were conducted using sliding speeds of 2.08 m/s, distances of 2000 m, and loads of 10–40 N. Experiments were run at constant loads of 40 N at velocities of 0.60, 1.20, 1.80, and 2.40 m/s. The steel disc was rotated at a constant speed while the test pin was held in place directly opposite the disc at all times. The weight of the test pins samples was determined precisely to within 0.0001 g using a digital electronic machine. Each test was followed by a thorough cleaning of the worn surface with acetone liquid. A test pin was used to compare the weight of the surface before and after wear. Using the gathered data, we were able to transform the weight loss information into volumetric wear loss.

3 Results and discussion

3.1 Microstructural analysis

Microphotographs of the SEM images of Al7010 alloy, Al7010 with 4 and 8 wt.% B_4C composites are shown in Figures 4a–4c. The SEM image of Al7010 alloy can be seen in Figure 4a. This shows the distinct grain boundaries without the presence of any particles. There are no cavities

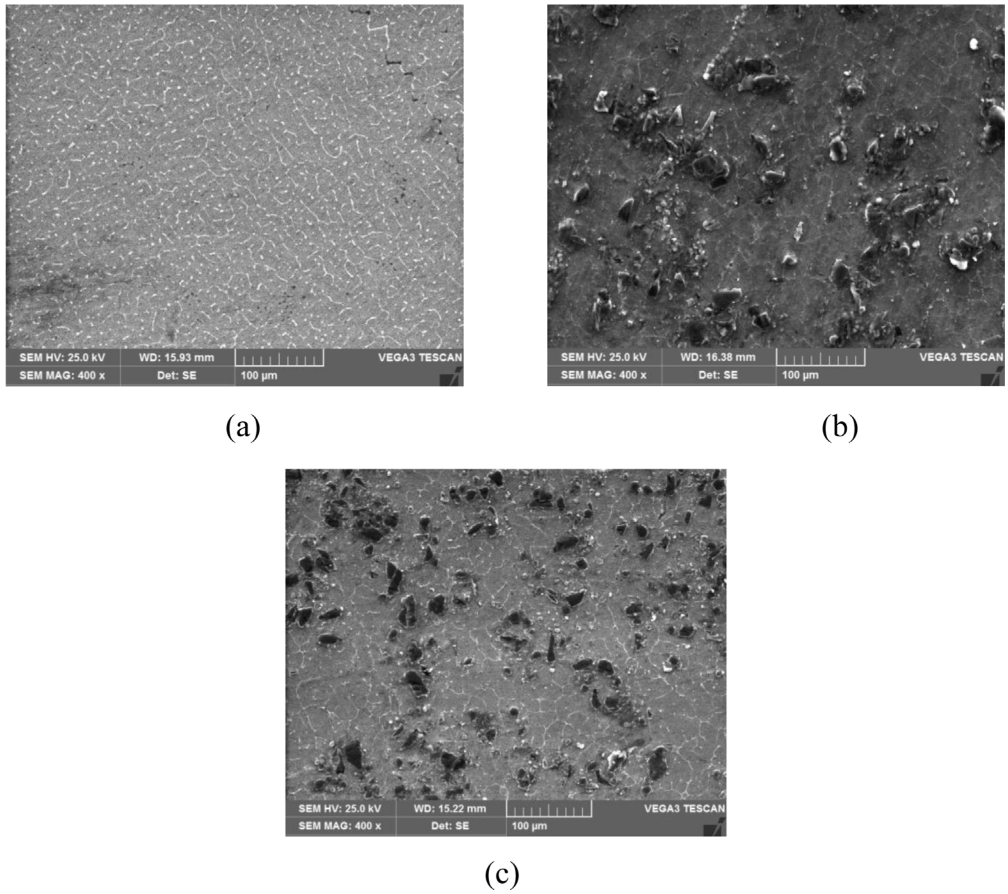

Fig. 4. SEM of (a) Al7010 alloy, (b) Al7010 with 4 wt.% B_4C, (c) Al7010 with 8 wt.% B_4C composites.

or other casting flaws visible on the micrograph. Figures 4b and 4c shows micrographs of Al7010-4 wt.% of B_4C, and Al7010-8 wt.% of B_4C composites. For B_4C reinforced composites, micro-particles can be clearly seen in the images taken with a microscope. By employing a novel, two-step stir casting route, these composites are free from clustering and agglomeration. Furthermore, the microstructure surface of Al7010 alloy with 8 wt.% B_4C composites microstructure contains many particles and also these are distributed throughout the Al7010 matrix.

A typical XRD pattern of Al7010 alloy is shown in Figure 5a, where various aluminium phases can be seen at various peaks. At 39, 45, 65, and 79, the occurrence of Al phases is confirmed with different intensities. At a wavelength of 39, the Al phase reaches its peak intensity. Al7010 alloy with 8% B_4C particulates reinforced composites is depicted in Figure 5b. Phases like Al and B_4C are shown in Figure 5b. As previously stated, there are numerous Al and B_4C particles phases existing at various 2 angles with varying intensities, as shown in the figure.

3.2 Density measurements

Figure 6 shows the density differences between the Al7010 and Al7010 with 4 and 8 wt.% B_4C composites. The rule of mixture is used to calculate the theoretical density of Al7010 alloy and B_4C composites. Furthermore, the weight concept is used to determine the experimental densities. In the study, B_4C particles had a density of 2.52 g/cc, which is lower than Al7010 alloy's theoretical density of 2.80. The density of the base alloy decreased from 2.80 g/cc to 2.775 g/cc as the wt.% of B_4C particles in the Al7010 matrix increased from 4 to 8 wt.%. Because B_4C particles have a lower density than Al matrix, their incorporation results in a decrease in density [17]. The overall density of the matrix is reduced as a result of the lower density of the reinforced particles. To make matters even more confusing, a quick glance at the graph shows that actual density values are only a tiny fraction of theoretical values.

3.3 Hardness measurements

Figure 7 depicts the hardness of Al7010 and Al7010 with B_4C micro particles composites. The hardness of Al7010 increases as the percentage of B_4C particles in the alloy increases from 4% to 8%, according to the plot. The hardness of Al7010 alloy is 65.5 BHN, in 4 wt.% of B_4C composites it is 81.3 BHN. Further, 8 wt.% of B_4C composites have 97.8 BHN. As the grain size of the filler is influenced by the presence of micro particles, an increase in hardness can be expected [18]. Adding micro particles to Al7010-B_4C composites can inhibit grain growth, progress crystal grains in the matrix, and have an impact on the refined composites.

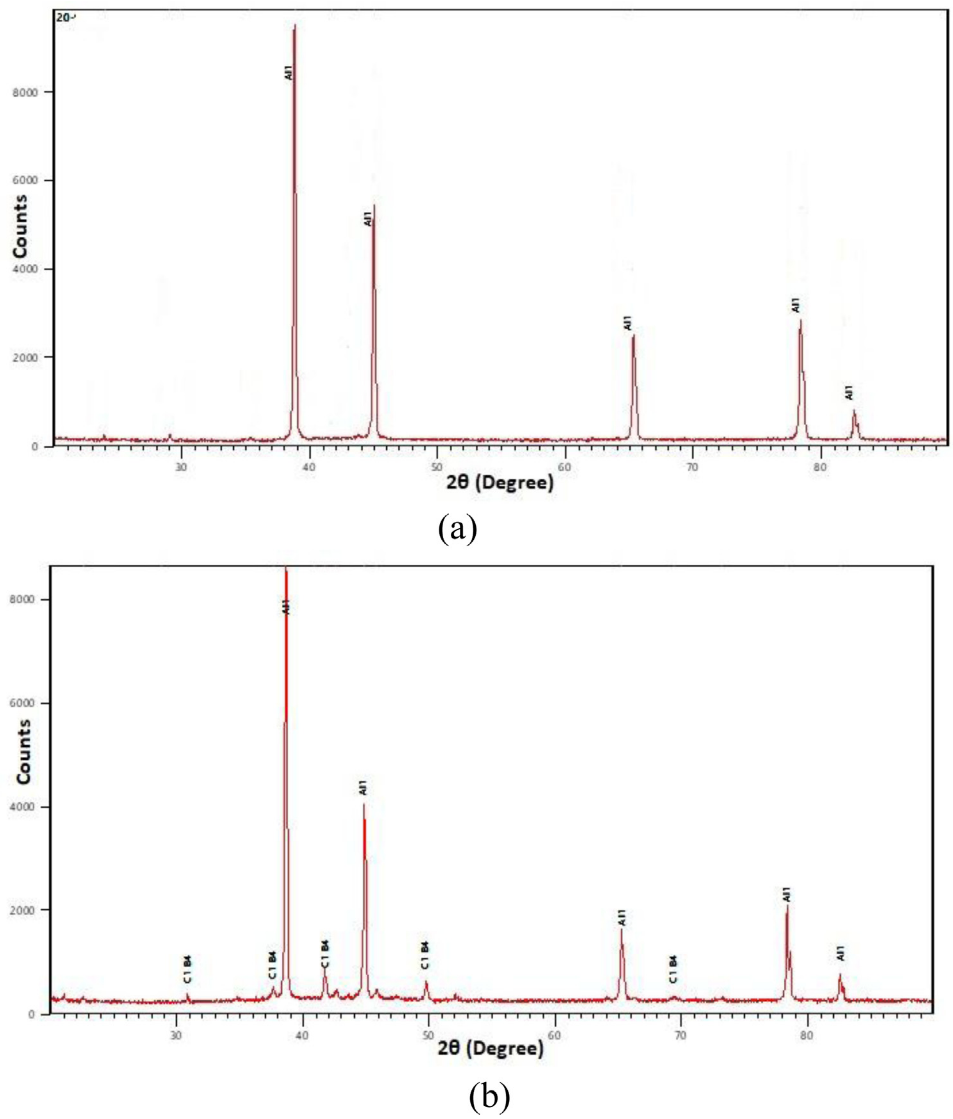

Fig. 5. X-ray diffraction patterns of (a) Al7010 alloy (b) Al7010-8 wt.% B_4C composites.

3.4 Ultimate tensile and yield strength

Figures 8 and 9 show the impact of B_4C particles with a diameter of 20–25 microns on the ultimate and yield strengths of an Al7010 alloy. Addition of B_4C has increased Al7010 alloy's tensile strength. This alloy has an ultimate and yield strength of 185.1 MPa and 147.2 MPa. Al7010 alloy with 8 wt.% B_4C particle composites has an ultimate and yield strength of 286 and 229 MPa, respectively. The strength of Al7010 has amplified more as the percentage of B_4C in the alloy increases from 4 to 8 wt.%.

The occurrence of micron-sized B_4C particles in the base Al7010 contributes to the alloy's increased strength. The thermal mismatch strain may follow up on the matrix as pre-stress, or it may discharge the disengagement loop and remove warm pressure. When the lattice material expands due to B_4C, it increases its dislocation density, which acts as a support effect on the Al network [19,20]. The Al7010 amalgam with B_4C composites is stronger as a result of the expansion in dislocation density. For composites made from aluminium alloys such as aluminium alloy Al7010, B_4C is a good choice because it acts as a barrier to particle dispersion and as a reinforcement of the matrix, preventing separation and improving the quality of the composites [21,22].

3.5 Percentage elongation

Figure 10 depicts the effect of 20–25 micron-sized B_4C particles on the Al7010 alloy's ductility. Al7010's ductility diminished as a result of B_4C particles. The presence of hard B_4C particles is to blame for this reduced ductility. As the B_4C content rises to 8 wt.%, the ductility decreases even more. The deformation of the Al7010 alloy matrix is limited by the presence of these particles.

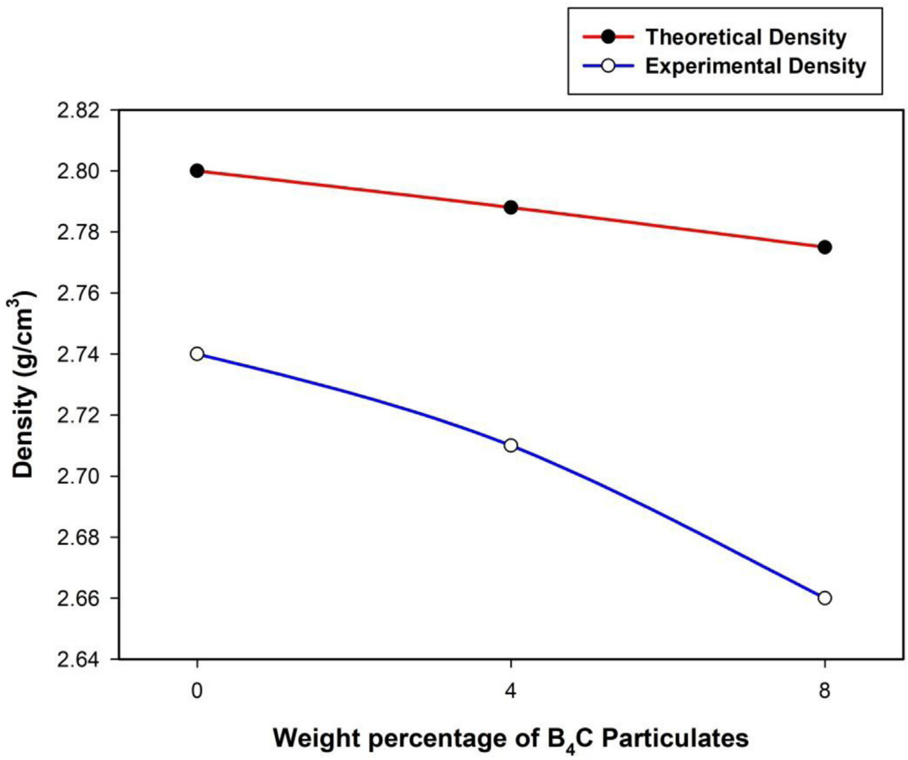

Fig. 6. Densities of Al7010 alloy with B_4C composites.

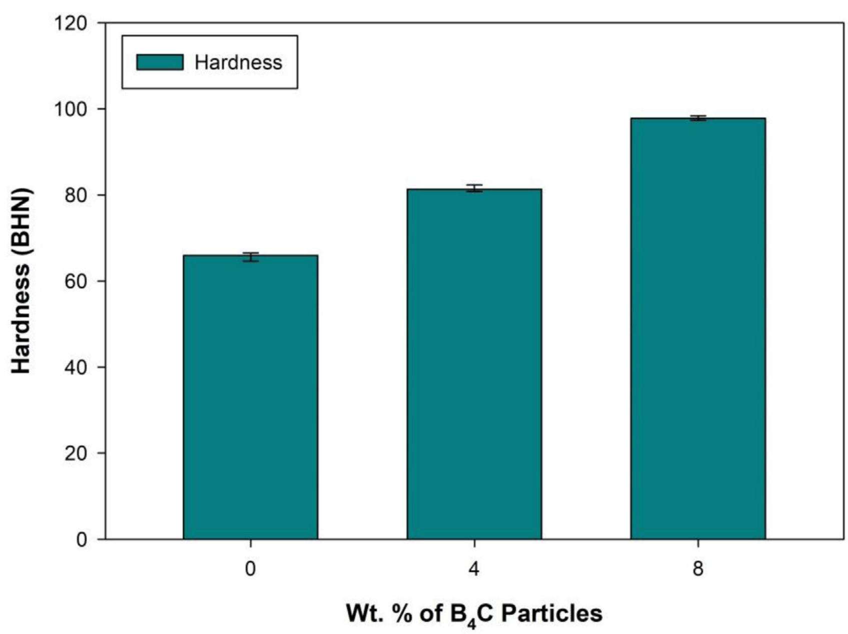

Fig. 7. Hardness of Al7010 alloy with B_4C composites.

3.6 Tensile fractography

Figure 11 depicts the fractured surfaces of Al7010 alloy and boron carbide composites made from it. An example of plastic fracture morphology is shown in Figure 11a. Al7010 fractures look like those shown in Figure 11a. An Al7010 alloy with 8 wt.% B_4C micro composites is depicted in Figure 11b. Al/B_4C composite dimple sizes and depths are altered when hard particles are added. Because of the brittle fracture morphology caused by boron carbide, this is a critical morphology indicator. Crack propagation along the interface of metal composites during the fracture process disperses a small quantity of particles at the edge of the dimple. Carbide particles in the Al7010 material cause the matrix to be more brittle when the mass fraction of carbide particles in the alloy increases.

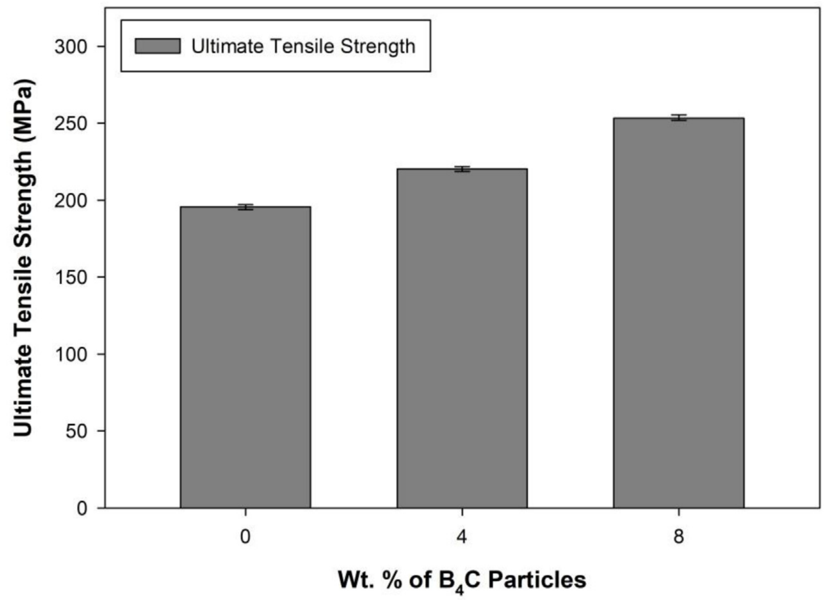

Fig. 8. Ultimate strength of Al7010 with B_4C composites.

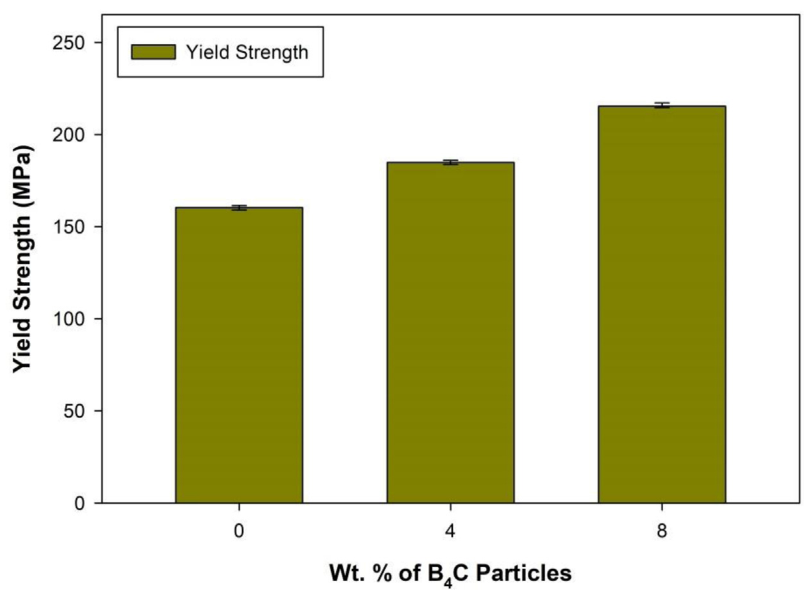

Fig. 9. Yield strength of Al7010 with B_4C composites.

3.7 Wear behaviour

3.7.1 Effect of load on volumetric wear loss

Al7010 alloy 20 to 25 micron sized B_4C composites volumetric wear loss at different loads of 10–40 N at constant speed of 2.40 m/s for 3000 m sliding distance is shown in Figure 12.

As can be seen in Figure 12, as the load on the specimen is increased from 10 N to 40 N, the wear of the Al7010 alloy also increases. It has been found that a load of 40 N causes the most material wear in all composites. At maximum load, the temperature of the sliding apparent and the pin rises above their critical level. As the load on the pin increases, the percentage of wear lost by the matrix and B_4C composites rises. However, it has been found that decreasing the wear loss of composites can be accomplished by adding 4 or 8 wt.% of B_4C reinforcements to the matrix alloy. Boron carbide particulates are a good barrier against material loss in composites due to their extreme hardness [23,24].

3.7.2 Effect of sliding velocity on volumetric wear loss

Al7010 alloy and 20–25 micron sized B_4C composites wear behavior at varying speeds of 0.60 m/s to 2.40 m/s at constant load of 40 N for 3000 m sliding distance is shown in Figure 13.

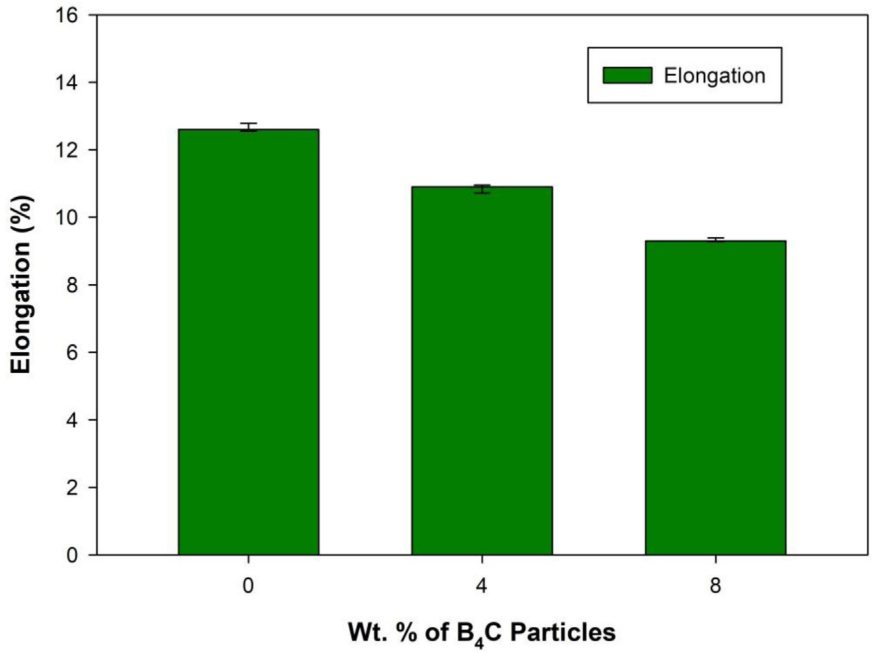

Fig. 10. Percentage elongation of Al7010 with B_4C composites.

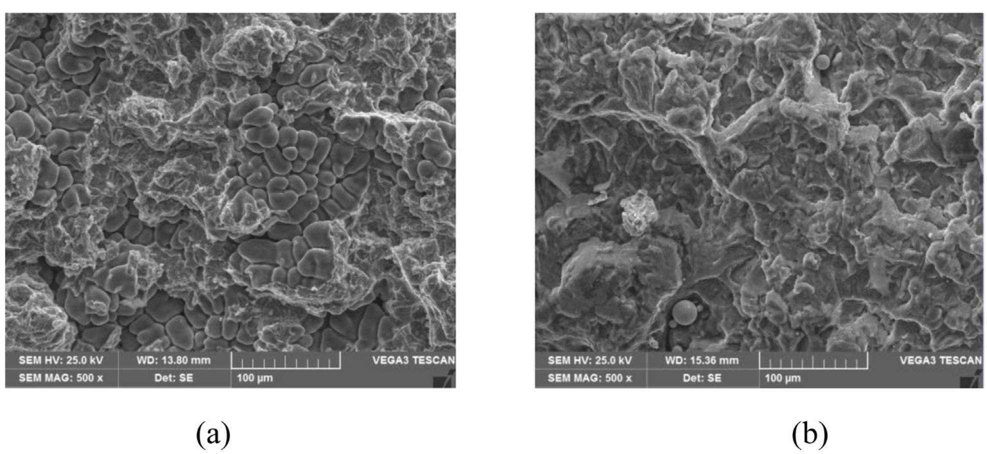

Fig. 11. SEM images of tensile fractured surfaces of (a) Al7010 alloy (b) Al7010 with 8 wt.% of B_4C composites.

A delamination in the Al7010 alloy has caused fragments of pins to be transferred to the disc, while larger pieces have been ejected [25,26]. Wear is decreased when B_4C is combined with Al7010. At the interface between the aluminium composite and the steel disc, B_4C particles form mechanically mixed layers that increase the wear resistance of the composite.

Volumetric wear loss is shown to be mild at lower sliding speeds of 0.60 m/s in Figure 13, but increases to moderate at 1.20 and 1.80 m/s, and to severe at 2.60 m/s for both the Al7010 alloy and all produced composites. The matrix and the composites should experience a rise in wear loss as a result. The increase in wear loss is primarily due to high strain deformation of the subsurface. When the rate of deformation below the surface increases, the areas where fractures and asperities fragment are created grow. Because of this, the volumetric wear loss and delamination are both increased. In addition, the softer composite brought on by the rubbing action at higher temperatures contributes more to the wear loss as sliding speed increases. As the temperature rises, the sliding speeds increase, causing the test piece to deform [27,28].

4 Conclusions

Stir technique was used to make Al7010 reinforced composites with B_4C particles of 20–25 micron size, with B_4C particle weight percentages ranging from 4 to 8 wt.%. The microstructure with density-hardness and tensile characteristics of Al7010 alloy metal composites were studied. SEM microphotographs show that the composites are free of pores and have a uniform distribution of micro particles. The XRD analysis shows that the Al7010 alloy

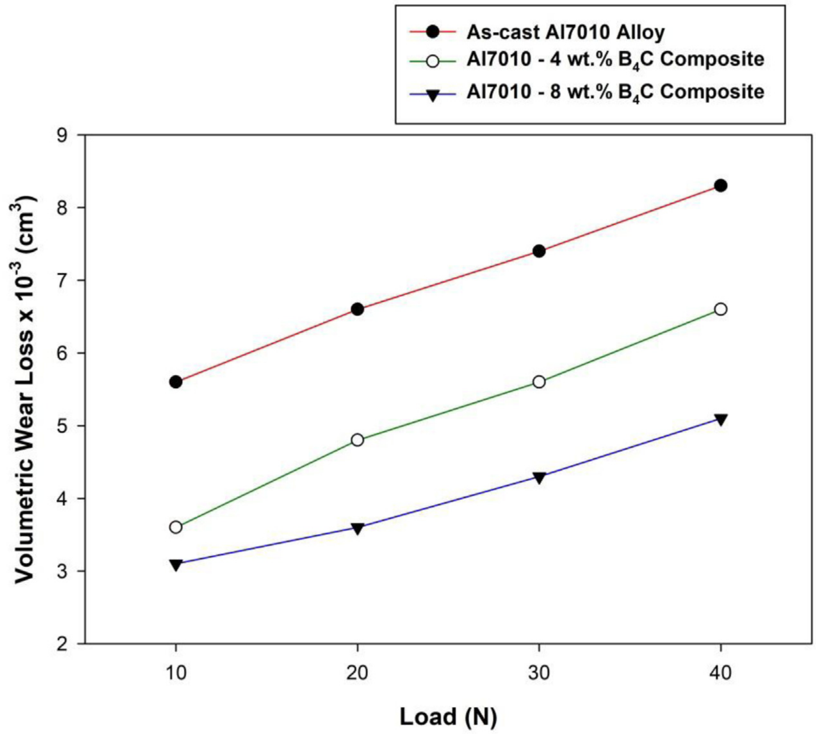

Fig. 12. Volumetric wear loss of Al7010 with micron sized B_4C composites at varying loads.

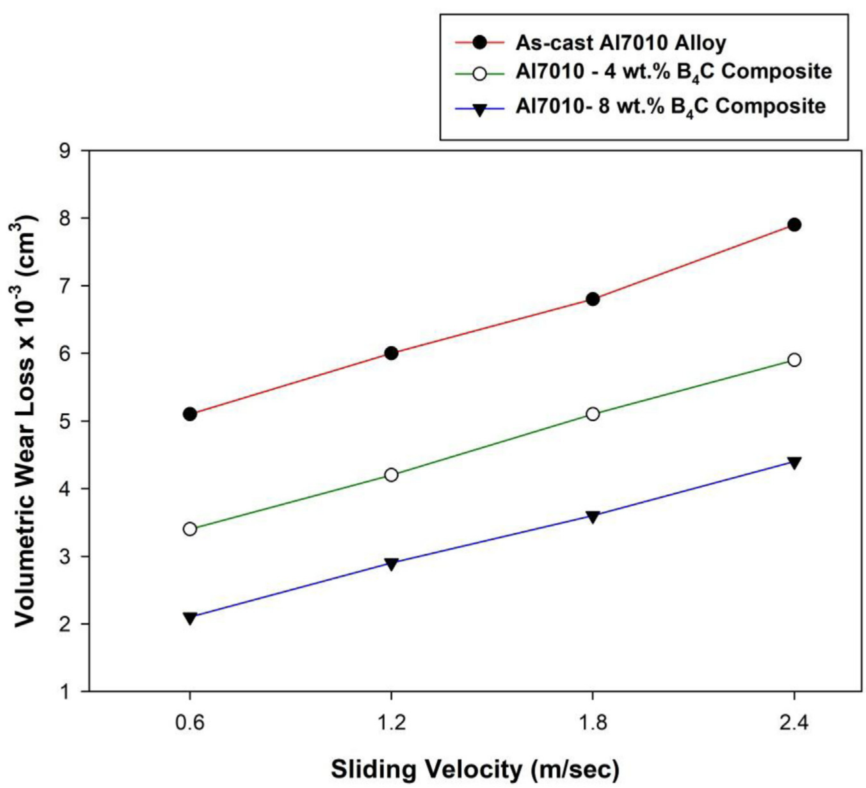

Fig. 13. Volumetric wear loss of Al7010 with micron sized B_4C composites at varying speeds.

matrix contains boron carbide particles. The B_4C particles reinforced composites outperformed the Al7010 alloy in terms of hardness and tensile strength. When related to the Al7010 alloy, metal composites had a slightly lower density. Using a tensile fractured surface as a guide, one can determine the nature of the fracture. Load and sliding speeds were impacted the wear behaviour of base Al7010 alloy and composites. Al7010 alloy with 8 wt.% of B_4C composites shows more wear resistance.

References

1. U.B. Krishna, B. Vasudeva, V. Auradi, M. Nagaral, Mechanical characterization and tensile fractography of Al7075-WCP-CoP composite, Frattura e Integrita Strutturale **16** (2022) 283–290
2. P. Shantharaj, A.S. Prashanth, M. Nagaral, V. Bharath, V. Auradi, K. Dharshan, Microstructure, tensile and compression behaviour of B_4C particles reinforced Al7075 matrix composites, Mater. Today: Proc. **52** (2022) 1135–1139
3. V. Bharath, V. Auradi, M. Nagaral, S. Babu Boppana, S. Ramesh, K. Palanikumar, Microstructural and wear behavior of Al2014-alumina composites with varying alumina content, Trans. Indian Inst. Metals **75** (2022) 133–147
4. V. Hiremath, V. Bharath, V. Auradi, S.T. Dundur, M. Nagaral, Machining of hard-to-cut materials: impact of varying weight proportion of boron carbide particle addition on cutting force and surface roughness of Al6061, J. Mater. Eng. Perform. **31** (2021) 3784–3791
5. H.S. Kumar, U.N. Kempaiah, M. Nagaral, V. Auradi, Impact, tensile and fatigue failure analysis of boron carbide particles reinforced Al-Mg-Si (Al6061) alloy composites, J. Failure Anal. Prevent. **21** (2021) 2177–2189
6. M. Nagaral, V. Auradi, V. Bharath, Mechanical characterization and fractography of 100 micron sized silicon carbide particles reinforced Al6061 alloy composites, Metall. Mater. Eng. **28** (2021) 17–32
7. U.B. Krishna, B. Vasudeva, V. Auradi, M. Nagaral, Effect of percentage variation on wear behaviour of tungsten carbide and cobalt reinforced Al7075 matrix composites synthesized by melt stirring method, J. Bio- Tribo-Corros. **7** (2021) 1–8
8. V. Bharath, V. Auradi, M. Nagaral, Fractographic characterization of Al_2O_3p particulates reinforced Al2014 alloy composites subjected to tensile loading, Frattura ed Integrità Strutturale **15** (2021) 14–23
9. S.B. Boppana, S. Dayanand, B. Vedashantha Murthy, M. Nagaral, A. Telagu, V. Kumar, V. Auradi, Development and mechanical characterisation of Al6061-Al_2O_3-graphene hybrid metal matrix composites, J. Compos. Sci. **5** (2021) 155
10. V. Bharath, D.H. Ashita, V. Auradi, M. Nagaral, Influence of variable particle size reinforcement on mechanical and wear properties of alumina reinforced 2014Al alloy particulate composite, FME Trans. **48** (2020) 968–978
11. W. Liao, B. Ye, L. Zhang, H. Zhou, W. Guo, Q. Wang, W. Li, Microstructure evolution and mechanical properties of SiC nanoparticles reinforced magnesium matrix composite processed by cyclic closed die forging, Mater. Sci. Eng. A **642** (2015) 49–56
12. C.S. Ramesh, R. Keshavamurthy, B.H. Channabasappa, A. Ahmed, Microstructure and mechanical properties of Ni-P coated Si3N4 reinforced Al6061 composites, Mater. Sci. Eng. A **502** (2009) 99–106
13. J. Harti, T.B. Prasad, M. Nagaral, K. Niranjan Rao, Hardness and tensile behavior of Al2219-TiC metal matrix composites, J. Mech. Eng. Autom. **6** (2016) 8–12
14. M. Nagaral, R.G. Deshapande, V. Auradi, S.B. Boppana, S. Dayanand, M.R. Anilkumar, Mechanical and wear characterization of ceramic boron carbide-reinforced Al2024 alloy metal composites, J. Bio- Tribo-Corros. **7** (2021) 1–12
15. T.H. Manjunatha, Y. Basavaraj, M. Nagaral, V. Venkataramana, Investigations on mechanical behavior of Al7075-nano B_4C composites, IOP Conf. Ser.: Mater. Sci. Eng. **376** (2018) 012091
16. G.B. Veeresh Kumar, G.V. Chowdary, M. Surya Vamsi, K. Jayarami Reddy, M. Nagaral, K. Naresh, Effects of addition of titanium diboride and graphite particulate reinforcements on physical, mechanical and tribological properties of Al6061 alloy based hybrid metal matrix composites, Adv. Mater. Process. Technolog. **8** (2021) 1–18
17. H.S. Kumar, U.N. Kempaiah, M. Nagaral, V. Auradi, Impact, tensile and fatigue failure analysis of boron carbide particles reinforced Al-Mg-Si (Al6061) alloy composites, J. Fail. Anal. Prevent. **21** (2021) 2177–2189
18. B.R. Mithun, M. Nagaral, V. Auradi, V. Bharath, Microstructure and mechanical properties of Cu coated Al_2O_3 particulate reinforced 6061 Al metal matrix composites, Mater. Today Proc. **4** (2017) 11015–11022
19. V. Balaraj, N. Kori, M. Nagaral, V. Auradi, Influence of Al_2O_3 and B_4C particles addition on the mechanical characterization of Al6061 alloy hybrid metal composites, Int. J. Vehicle Struct. Syst. **13** (2021) 624–629
20. B.N. Sarada, P.L. Srinivasa Murthy, G. Ugrasen, Hardness and wear characteristics of hybrid aluminium metal matrix composites produced by stir casting technique, Mater. Today Proc. **2** (2015) 2878–2885
21. G. Veeresha, B. Manjunatha, V. Bharath, M. Nagaral, V. Auradi, Synthesis, microstructural characterization, mechanical, fractographic and wear behavior of micro B_4C particles reinforced Al2618 alloy aerospace composites, Frattura e Integrita Strutturale **62** (2022) 385–407
22. S. Krishna Prasad, S. Dayanand, M. Rajesh, M. Nagaral, V. Auradi, R. Selvaraj, Preparation and mechanical characterization of TiC particles reinforced Al7075 alloy composites, Adv. Mater. Sci. Eng. (2022) 7105189
23. N. Kumar, H.S. Kumar, T.H. Raju, Microstructural characterization, mechanical and Taguchi wear behavior of micro-titanium carbide particle-reinforced Al2014 alloy composites synthesized by advanced two-stage casting method, J. Bio Tribo-Corros. **8** (2022) 109
24. V. Anjan Babu, V. Auradi, M. Nagaral, Mechanical and wear characterisation of boron carbide particles reinforced Al2030 alloy composites developed by two stage stir cast method, Adv. Mater. Process. Technolog. **8** (2022) 1–15
25. S. Matti, B.P. Shivakumar, M. Nagaral, S. Shashidhar, P. N. Siddappa, V. Auradi, Mechanical and tribological behavior of flyash, red mud and mica particles reinforced Al7075 alloy hybrid metal composites, Manufactur. Rev. **9** (2022) 11
26. R. Kumar, R.G. Deshpande, B. Gopinath, J. Harti, M. Nagaral, V. Auradi, Mechanical fractography and worn surface analysis of nanographite and ZrO_2-reinforced Al7075 alloy aerospace metal composites, J. Failure Anal. Prevent. **21** (2021) 525–536

27. S. Attar, M. Nagaral, H.N. Reddappa, V. Auradi, Effect of B_4C particulates addition on wear properties of Al7025 alloy composites, Am. J. Mater. Sci. **5** (2015) 53–57
28. M. Nagaral, V. Auradi, K.I. Parashivamurthy, B.K. Shivananda, S.A. Kori, Dry sliding wear behaviour of aluminium 6061-SiC-graphite particulates reinforced hybrid composites, IOP Conf. Ser.: Mater. Sci. Eng. **310** (2018) 012156

Cite this article as: Kotresha Mydur, Mahendra Kumar S., Madeva Nagaral, Virupaxi Auradi, Bharath V., Sudarshan T.A., Microstructure, physical, tensile and wear behaviour of B_4C particles reinforced Al7010 alloy composites, Manufacturing Rev. **10**, 3 (2023)